Tutor/s

Dr. Josep Puigmartí-Luis
Departament de Ciència de Materials i Química Física

Dr. Alessandro Sorrenti
Departament de Química Inorgànica i Orgànica

James D. Nicholas
Departament de Ciència de Materials i Química Física

Grau de Química

Treball Final de Grau

Development of a redox active colloidal system for dissipative self-assembly.

Desenvolupament d'un sistema col·loidal amb activitat redox per l'autoassemblatge dissipatiu.

Gemma Llauradó Capdevila

June 2021

UNIVERSITAT DE BARCELONA

B:KC Barcelona Knowledge Campus
Campus d'Excel·lència Internacional

Nothing in life is to be feared, it is only to be understood. Now is the time to understand more, so that we fear less.

Marie Curie

En primer lloc, m'agradaria agrair al grup de recerca ChemInFlow per haver-me permès realitzar aquest projecte. Voldria agrair especialment als meus supervisors, Dr. Josep Puigmartí-Luis, Dr. Alessandro Sorrenti i James Nicholas, per la seva disposició, guia i suport en tot moment. També voldria agrair a la resta de l'equip per la bona acollida i per haver-me donat l'oportunitat de gaudir d'aquest treball.

REPORT

CONTENTS

1. SUMMARY

Dissipative self-assembly (DSA) is a process that leads to the formation of structures and materials away from the thermodynamic equilibrium state through a controlled exchange of energy and/or matter with the environment[1]. This form of self-assembly is key in numerous biological processes, and, in living organisms, it enables properties such as self-healing, self-replication, signal processing and motility, among others. Recently, there is a growing interest in developing synthetic supramolecular and colloidal systems that can undergo dissipative self-assembly, for example controlled by the consumption of chemical fuel(s).

The overall goal of this TFG project is to develop a colloidal system based on ferrocene-functionalized silica (SiO_2) particles whose assembly can be controlled via redox-responsive host-guest interactions between the ferrocene (Fc) moiety and a β-cyclodextrin-dimer that can act as a linker between the particles. The addition of suitable chemical fuels (an oxidant and a reductant) will allow us to regulate the assembly/disassembly of the colloidal system, which depends on the kinetics of the redox process.

To achieve this goal, monodisperse non-fluorescent and fluorescent core-shell SiO_2 particles were synthesized, and subsequently functionalized with Fc moieties using 'click' chemistry. Full physicochemical and size characterization of the particles proved the success of the synthesis and functionalization steps, demonstrating the formation of spherical, monodisperse Fc-functionalized particles with size around 500 nm. Redox kinetic studies with a variety of oxidants and reductants were performed using molecular ferrocene, in order to optimize the experimental conditions to be used for the dissipative self-assembly. These studies showed that $FeCl_3$ and ascorbic acid are the most suitable pair of redox agents for fast redox switching of Fc, whilst H_2O_2 is more suitable for fine-tuning the redox kinetics. Preliminary self-assembly studies revealed that in the presence of β-cyclodextrin-dimer, Fc-functionalized particles assemble, and could then be disassembled by addition of an oxidant. This result is promising for the development of DSA, and further studies are being carried out to investigate this system in more depth.

Keywords: Dissipative self-assembly, Redox active colloids, Colloidal assembly, Supramolecular chemistry

2. RESUM

L'autoassemblatge dissipatiu (DSA) és un procés que condueix a la formació d'estructures i materials allunyats de l'estat d'equilibri termodinàmic mitjançant un intercanvi controlat d'energia i/o matèria amb l'entorn[1]. Aquesta forma d'autoassemblatge és clau en nombrosos processos biològics i, en els organismes vius, atorga propietats com l'autocuració, l'autoreplicació, el processament del senyal i la motilitat, entre d'altres. Recentment, hi ha un augment d'interès en el desenvolupament de sistemes sintètics supramoleculars i col·loidals que puguin experimentar un assemblatge dissipatiu, per exemple, controlats pel consum de combustible(s) químic(s).

L'objectiu general d'aquest projecte de TFG és desenvolupar un sistema col·loidal basat en partícules de sílice (SiO_2) funcionalitzades amb ferrocè (Fc), l'assemblatge dels quals pugui ser controlat mitjançant interaccions amfitrió-hoste sensibles a l'activitat redox entre la unitat de ferrocè i un dímer de β-ciclodextrina, que pot actuar com un enllaç entre les partícules. L'addició de combustibles químics adequats (un oxidant i un reductor) ens permetrà regular l'assemblatge/ desassemblatge del sistema col·loidal, que depèn de la cinètica del procés redox.

Per assolir aquest objectiu, es van sintetitzar partícules monodisperses de SiO_2 amb nucli fluorescent i no fluorescents i, posteriorment, es van funcionalitzar amb unitats de Fc mitjançant la química 'clic'. La completa caracterització fisicoquímica i de mida de les partícules va confirmar l'èxit dels passos de síntesi i de funcionalització, demostrant la formació de partícules esfèriques, monodisperses, funcionalitzades amb Fc d'uns 500 nm de mida. Estudis sobre la cinètica redox van ser realitzats amb diversos oxidants i reductors mitjançant ferrocè molecular, per tal d'optimitzar les condicions experimentals utilitzades per a l'autoassemblatge dissipatiu. Aquests estudis van demostrar que el $FeCl_3$ i l'àcid ascòrbic són el parell d'agents redox més adequats per a la commutació ràpida del procés redox del Fc, mentre que l'H_2O_2 és més adequat per afinar la cinètica redox. Els estudis preliminars d'autoassemblatge van indicar que, en presència del dímer β-ciclodextrina, les partícules funcionalitzades amb Fc s'agreguen, i podrien desassemblar-se mitjançant l'addició d'un oxidant. Aquest resultat és prometedor pel desenvolupament de processos DSA, i s'estan duent a terme estudis addicionals per tal d'investigar aquest sistema amb més profunditat.

Paraules clau: Autoassemblatge dissipatiu, Col·loides redox actius, Assemblatge col·loidal, Química supramolecular

3. INTRODUCTION

3.1. DISSIPATIVE SELF-ASSEMBLY

Equilibrium self-assembly is a process in which a disordered ensemble of molecular or colloidal building blocks organizes into an ordered superstructure as a consequence of the interactions between them.[2] This is a spontaneous process governed by thermodynamic stability, and thus, it does not require the presence of any fuel or external agent to proceed. Simply, the system evolves naturally to the lowest energy state (Figure 1A).

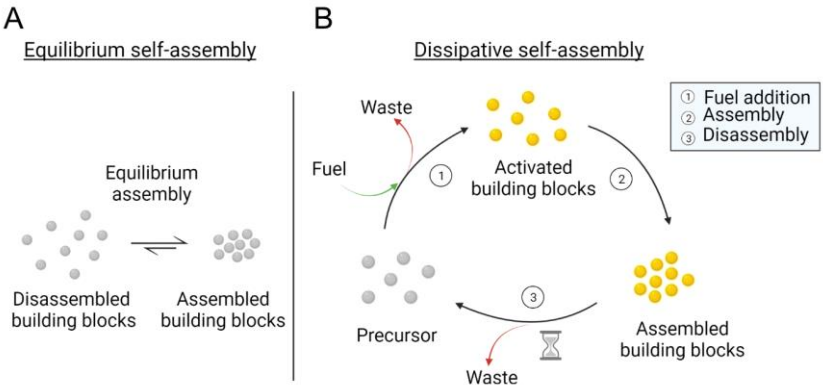

Figure 1. Representation of (A) Equilibrium self-assembly versus (B) Dissipative self-assembly.

However, other types of self-assembly exist in nature. For instance, living organisms commonly make use of the so-called dissipative self-assembly, which is the process we have focused on for this project.

Dissipative self-assembly is a process that relies on energy consumption (Figure 1B). Typically, this energy is provided by the addition of one (or more) chemical fuels to activate the building blocks. The supplied energy is thus used to promote the self-assembly process, while part of the energy is also dissipated by waste formation. In addition, a deactivation step (which may require an additional fuel) is needed to slowly bring the assembled system back to its original non-assembled state. Therefore, in DSA, the composition of the system is not dictated by the

relative thermodynamic stability of the assembled and disassembled states, but rather on the kinetic of the activation/deactivation reactions. This provides temporal control over the assembled structures. The assembled states obtained by DSA thus correspond to non-equilibrium states, which do not lie in global or local minima of the free-energy landscape.[1–3]

Numerous examples of DSA can be found in nature, more specifically in biological systems. A well-known example is the reversible formation of actin filaments, where the ATP (adenosine triphosphate) fuel is used to keep the assembled structure away from thermodynamic equilibrium.[1,3]

3.2. SYNTHETIC COLLOIDAL SYSTEMS

A colloidal system is defined as a mixture in which dispersed particles remain suspended in a continuous medium. Thus, two phases are identified: the suspended particles (dispersed phase) and the medium (continuous phase). Colloidal particles have been used as building blocks for the bottom-up preparation of organized structures and materials for different applications, such as self-erasing images, temporary data storage, and switchable catalytic activities, among others.[2] This is due to the possibility to control interparticle interactions through facile surface-functionalization. A large number of self-assembling colloids have been prepared. Among them, stimuli-responsive colloidal systems whose equilibrium self-assembly can be controlled by a wide range of stimuli including pH, temperature, light, and redox reactions.[2,4]

For example, Vilanova and co-workers have studied the colloidal assembly triggered by UV-light. In this work, silica microparticles were functionalized with a photo-responsive supramolecular moiety, namely a hydrogen bonding benzene-1,3,5-tricarboxamide (BTA) unit bearing a photolabile protecting group. The irradiation with UV-light removes the protecting group enabling the formation of H-bonds between particles, thus promoting their self-assembly.[5]

Other authors have reported on the non-equilibrium dissipative self-assembly of colloidal particles both driven by light or by the consumption of chemical fuels. For example, Klajn and co-workers showed that the conformational change of azobenzene moieties on the surface of gold and silver nanoparticles promoted by UV irradiation results in light mediated DSA of the colloidal system used to make self-erasing images.[6] Van Ravensteijn and co-workers reported on polymer-grafted particles capable of undergoing transient assembly upon addition of a strong methylating agent (dimethyl sulfate) as the chemical fuel.[7]

3.3. FERROCENE-CYCLODEXTRIN HOST-GUEST INTERACTIONS

In supramolecular chemistry host-guest interactions occur between two or more molecules that have a special structural relationship and are held together by multiple non-covalent forces, such as hydrogen-bonding, π−π stacking interactions, electrostatic interactions, van der Waals forces and hydrophobic interactions.[8] In a host-guest complex, the 'host' is typically the larger molecule that recognizes and binds non-covalently one or a few smaller 'guest' molecules, in a way that resembles the formation of enzyme-substrate complexes.

Cyclodextrins (CD) are water-soluble cyclic oligomers of glucose (with six, seven or eight glucose units, called α-, β-, and γ-CD respectively), which have been largely used as macrocyclic host molecules due to their tendency to form stable 1:1 inclusion compounds with a variety of apolar guest molecules. In the past, CDs have been studied as catalysts, usually in aqueous media, and as enzyme models, since the formation of their inclusion complexes mimics the Michaelis-Menten complex formation in enzyme reactions.[9] However, in the last decades the focus of studies with CDs has shifted to their incorporation in functional supramolecular and polymeric materials, where they can enable functionalities such as molecular recognition, hydrolysis, catalysis, and polymerization.[10]

In particular, cyclodextrins are excellent hosts for ferrocene (Fc) in its reduced neutral form, forming a 1:1 complex in which the Fc unit enters in the CD cavity as driven by strong hydrophobic interactions,[11] with an association constant (k_a) of $4.1 \cdot 10^3$ M^{-1} in water.[12] However, such complex cannot be formed with oxidized Fc, i.e. with the ferrocenium (Fc^+) ion, which is hydrophilic. Thus, if the Fc moiety is oxidized when bound inside the CD cavity, the hydrophobic interactions are weakened, which induces the complex dissociation (Figure 2).

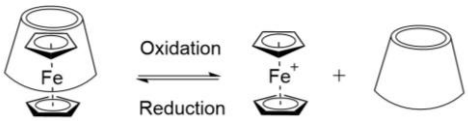

Figure 2. Representation of the redox-responsive Fc-β-CD host-guest interaction.

This property has been largely exploited to build redox-responsive supramolecular and polymeric systems,[13] including redox-switchable supramolecular polymers,[14] stimuli responsive drug delivery systems,[15] and self-healing hydrogels.[16,17]

3.4. OUR SYSTEM

In this TFG project, ferrocene functionalized silica particles will be prepared and studied as candidate building blocks for dissipative colloidal assembly (Figure 3). Fc-functionalized silica particles will interact with a ditopic linker, a β-cyclodextrin dimer (β-CD-dimer), which will enable the colloidal assembly to take place (Figure 3). The driving force for the colloidal assembly is thus the supramolecular host-guest interaction between ferrocene and β-cyclodextrin.[12]

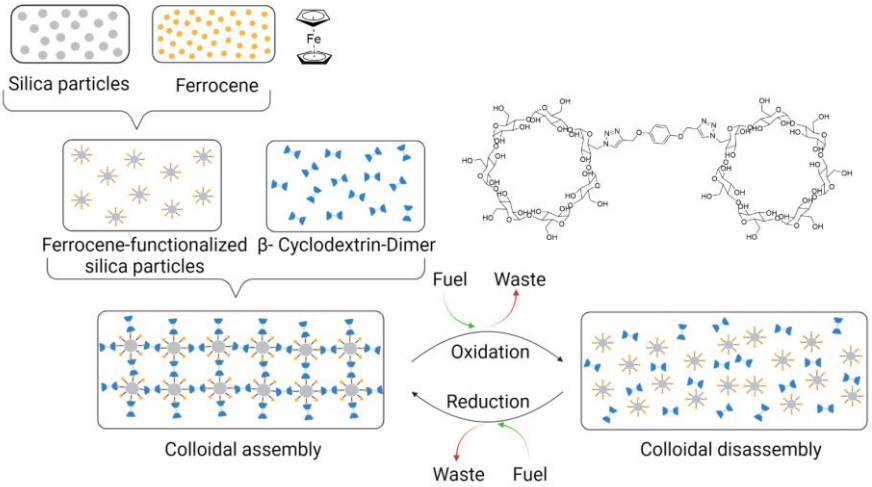

Figure 3. Schematic representation of dissipative colloidal assembly controlled by redox-switchable host-guest interactions that will be studied in this TFG project.

Two redox fuels, an oxidant and a reductant, can be used to control the disassociation and reassociation of the Fc/β-CD complex, which in turn will allow us to control the colloidal disassembly and reassembly depending on the kinetics of the redox processes.

4. OBJECTIVES

The overall goal of this project is the design and preparation of a colloidal system whose assembly can be controlled by redox-switchable host-guest interactions in the presence of suitable chemical fuels (an oxidant and a reductant). To achieve this overall goal, the following tasks must be performed:

- Synthesis of monodisperse non-fluorescent and fluorescent core-shell SiO_2 particles via the Stöber method;
- Functionalization of the particles with an azide-containing chain followed by functionalization with redox-active ferrocene units via 'click' chemistry;
- Particle size characterization by Dynamic Light Scattering (DLS) and Scanning Electron Microscopy (SEM);
- Physicochemical characterization of the functionalized SiO_2 particles by different techniques;
- Investigation of the redox behavior of ferrocene in the presence of various oxidants and reductants, and study of the redox kinetics;
- Study of the colloidal assembly by Bright Field and Fluorescence Microscopy.

5. RESULTS AND DISCUSSION

5.1. SYNTHESIS OF FERROCENE-FUNCTIONALIZED SILICA PARTICLES

5.1.1. Synthesis of SiO_2 particles

Non-fluorescent and fluorescent silica particles were synthesized through the Stöber method.[18–20] This is a sol-gel process commonly used to obtain spherical, monodisperse, SiO_2 particles with controlled size starting from the molecular precursor tetraethyl orthosilicate (TEOS). In particular, we followed an adapted two-step synthetic protocol for the preparation of the particles,[21] involving first the formation of seeds of around 200 nm (step 2 in Scheme 1), which were isolated and fully characterized, followed by their further growth induced by continuous addition of the TEOS precursor and ammonium hydroxide (step 3 in Scheme 1).

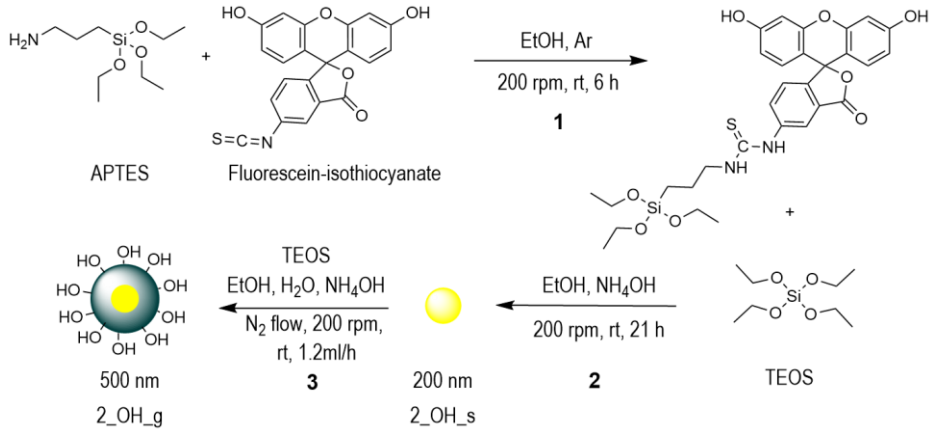

Scheme 1. Preparation of fluorescent SiO_2 particles. (1) Synthesis of dye-functionalized APTES precursor; (2) Synthesis of fluorescent SiO_2 seeds **2_OH_s**; (3) Synthesis of core-shell SiO_2 particles **2_OH_g**.

For the preparation of the fluorescent seeds, we first prepared a dye-functionalized precursor by reaction of fluorescein-isothiocyanate with 3-aminopropyltriethoxysilane (APTES) in ethanol (step 1 in Scheme 1). This fluorescein-APTES precursor was then used together with TEOS in the Stöber process for the preparation of the seeds (step 2 in Scheme 1). The obtained fluorescent

seeds **2_OH_s** were then subjected to a growing step (step 3 in Scheme 1) leading to core-shell SiO_2 particles **2_OH_g**. An analogous two-step procedure was used to prepare first non-fluorescent SiO_2 seeds **1_OH_s** and eventually grown SiO_2 particles **1_OH_g**.

Hydrolysis and condensation reactions take place during the synthesis. To accelerate the polycondensation reaction, ammonium hydroxide is required in order to increase the pH, which results in faster condensation. It has been demonstrated that the concentration of ammonium hydroxide plays a crucial role in determining the final particle size. The greater the concentration, the bigger the particle size, until a plateau is reached.[19] Besides, the role of ammonium hydroxide is to generate repulsive charges between the forming silica particles (negatively charged), which eventually leads to monodispersity. Therefore, we performed preliminary tests varying the concentration of ammonium hydroxide between 0.18 and 2 M in order to optimize the size of the formed seeds. Since we found that the seeds formed at the lower concentrations were too small and difficult to isolate by centrifugation, we chose to continue using higher ammonium hydroxide concentrations (Table 1).

Sample	NH_4OH [mol/L]	TEOS [mol/L]	Temperature (°C)	Time (h)
1_OH_s	1.14	0.15	rt	17
2_OH_s	1.96	0.15	rt	21

Table 1. Parameters chosen for the synthesis of SiO_2 seeds.

An increase of the turbidity of the reaction mixture was observed along the course of the reaction due to light scattering by the particles (Tyndall effect) as shown in Figure 4A and B.

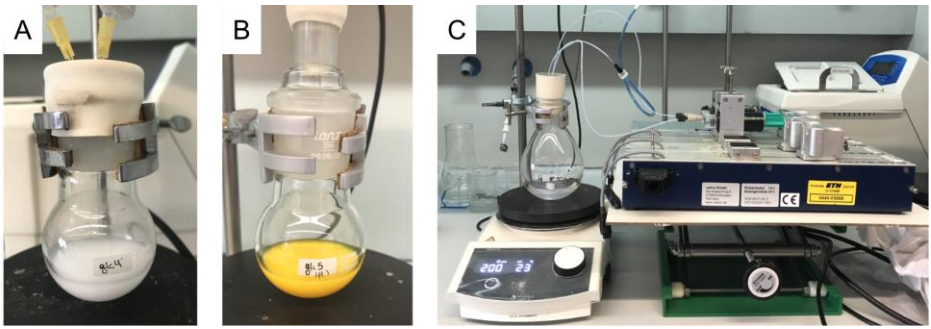

Figure 4. Pictures of (A) non-fluorescent seeds formed in the reaction mixture; (B) fluorescent seeds in the reaction mixture; (C) set-up used for the synthesis of core-shell particles (growing step).

In the growing step, leading to core-shell particles, the particle growth was controlled by continuous and simultaneous infusion of the TEOS precursor (in ethanol) and ammonium hydroxide (in ethanol/water) into an ethanolic dispersion of the seeds by using syringe pumps (Figure 4C). An inert atmosphere was provided through a continuous N_2 flow to avoid contact between the ammonia vapors and the outlet delivering the TEOS, which could result in secondary nucleation. This set-up allowed us to control the delivery of the reactants by controlling the flow rates of addition, thus controlling the reaction rate, and avoiding further nucleation (see Experimental Section). Particles of around 400-500 nm were obtained in this step.

5.1.2. Functionalization of SiO_2 particles

A two-step synthetic route was used for preparing ferrocene-functionalized silica particles both with a non-fluorescent and fluorescent core, **1_Fc** and **2_Fc** respectively (Scheme 2). In the first step we prepared azide-functionalized SiO_2 particles by condensation reaction of the grown bare SiO_2 particles (**1_OH_g**, **2_OH_g**) with 3-azidopropyltriethoxysilane to give **1_N_3** and **2_N_3** respectively (1a or 1b in Scheme 2). The ferrocene was then introduced at the surface of the particles by copper-catalyzed 'click' reaction with ethynylferrocene.

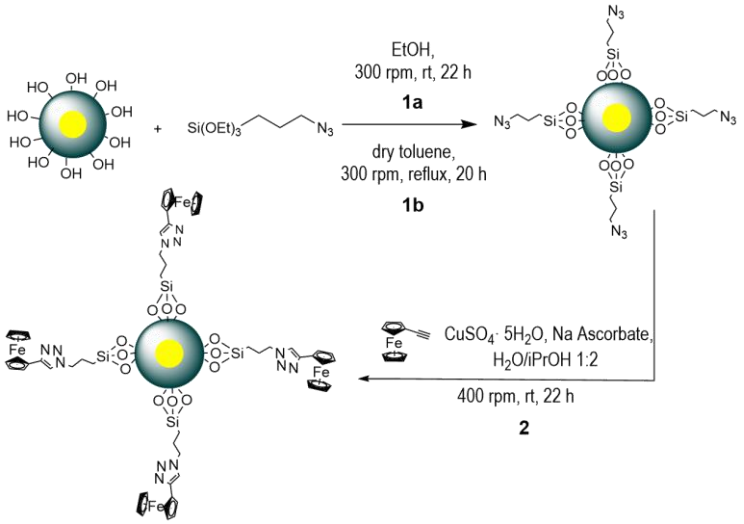

Scheme 2. Functionalization of SiO_2 particles. (1a) Synthesis of azide-functionalized SiO_2 particles in ethanol; (1b) Synthesis of azide-functionalized SiO_2 particles in toluene; (2) Synthesis of ferrocene-functionalized SiO_2 particles by click-reaction.

For the preparation of azide-functionalized particles we tested different reaction conditions, adapting previously reported methods. Namely, the condensation reaction was performed either in ethanol at room temperature[22] or in dry toluene at reflux[23] (1a and 1b in Scheme 2 respectively). The exact conditions used are reported in the Experimental Section. In the case of fluorescent particles **2_OH_g** only the condensation in ethanol in mild conditions was performed to prevent the possible degradation of fluorescein and consequent loss of the particle's fluorescence. All of the azide-functionalized silica particles were separated from the reaction mixture by centrifugation, washed three times and dried before the next step.

The ferrocene moiety was attached to the particle through copper catalyzed Huisgen type [3+2] azide–alkyne cycloaddition (CuAAC) in a water/isopropanol mixture, leading to the formation of a stable triazole linker.[24] In particular, the Cu(I) catalyst was generated in situ by reducing $CuSO_4$ using sodium ascorbate (2 in Scheme 2). The 'click' route was chosen because of its high efficiency, requirement of mild reaction conditions and absence of side products.[23] The amount of ethynylferrocene to add to the reaction mixture was calculated on the basis of an estimation of the number of $-N_3$ groups per total surface area of the particles. This was done by assuming that one molecule covered 0.6 nm^2 of the surface of the particle,[22] and using the volume/area of the particles calculated from their radius obtained by SEM measurements (see below).

The Fc-functionalized particles were separated from the reaction mixture by centrifugation, and first washed with EDTA to remove any remaining copper salts, and then with H_2O and ethanol leaving a yellow-orange precipitate, indicating the presence of ferrocene on the particles.

5.2. CHARACTERIZATION OF THE SILICA PARTICLES

5.2.1. Particle size characterization

The size and size distributions of the seeds and grown SiO_2 particles, for both non-fluorescent (**1**) and fluorescent (**2**) samples were measured by two different techniques, Dynamic Light Scattering and Scanning Electron Microscopy. This allowed us to assess the success of the two-step synthesis of the core-shell particles. The results are summarized in Table 2. DLS measurements were carried out in a quartz cuvette containing the recently dispersed colloid in ethanol. The values obtained for the hydrodynamic diameter (d_H) indicate that both the seeds and grown particles have a high degree of monodispersity and show no significant aggregation in the

timescale of the measurement. In particular, the polydispersity index (PDI), calculated as the square of the standard deviation divided by the square of the mean, is less than 0.2 in all the samples (Table 2).

	Seeds			Core-shell			Ferrocene
	Particle size (nm)			Particle size (nm)			Particle size (nm)
Sample	DLS	SEM	PDI*	DLS	SEM	PDI*	SEM
1	181 ± 74	174 ± 22	0.16	519 ± 26	392 ± 19	0.003	410 ± 16
2	253 ± 43	188 ± 11	0.03	696 ± 111	489 ± 19	0.03	472 ± 12

(1) Non-fluorescent
(2) Fluorescent

*calculated from the DLS data

Table 2. Summary of particle size analysis results.

SEM imaging of the colloidal dispersions drop cast on glass allowed us to observe the particle morphology, confirming the presence of monodisperse homogeneous spherical particles in all the investigated samples (Figure 5A and B, and Appendix 1). Image analysis was performed using Image J, to estimate the particle size distribution for the different samples (Figure 5C and D, and Appendix 2). We used more than 100 particles measured from different images for this analysis.

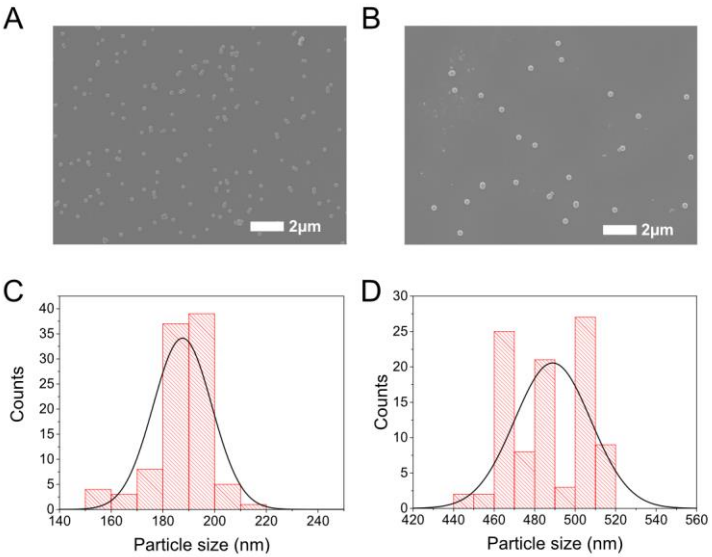

Figure 5. (A) and (B) SEM images of **2_OH_s** and **2_OH_g** respectively; (C) and (D) size distribution obtained from the image analysis of samples of **2_OH_s** and **2_OH_g** respectively.

The size distribution of the SiO_2 particles was plotted as an histogram and fit to a Gaussian function which allowed us to determine the average diameter (Figure 5C and D).

We should point out that the values of particle size obtained by DLS measurements tend to be slightly higher than the ones calculated by SEM image analysis. This is unsurprising since DLS measures the hydrodynamic diameter of the particles which may differ significantly from their physical size.[25] In addition, the minor presence of small particle aggregates (dimers, trimers) can have a significant influence on the DLS measurement leading to overestimation of the average particle size.

Overall, the DLS and SEM results confirmed that the two-step synthesis proceeded successfully producing seeds of around 200 nm in diameter and grown core-shell particles between 400 and 500 nm, depending on the sample.

5.2.2. Physicochemical characterization of the SiO_2 particles

Fluorescence measurements were performed on ethanol dispersions of both non-fluorescent **1_OH_g** and fluorescent **2_OH_g** particles. The fluorescence spectra revealed the presence of an emission band centered at 520 nm only in the case of **2_OH_g**, thus indicating that the fluorescein chromophore molecule was successfully incorporated in the core of the SiO_2 particles (Figure 6A).

FT-IR spectroscopy was employed to verify the successful functionalization of the particles with both the azide group and the ferrocene moiety. Unfortunately, we did not observe clear changes in the spectra in comparison with the bare unfunctionalized particles (see Appendix 3). For example, the characteristic azide group stretching band at around 2100 cm^{-1} was not clearly visible. This may be attributed to the fact that big SiO_2 particles (hundreds of nanometers) have a low surface to volume ratio, resulting in a low concentration of $-N_3$ groups with respect to the bulk SiO_2 material.[25]

However, the success of the Fc-functionalization through the 'click' reaction could be clearly inferred by the yellow-orange color assumed by the **1_Fc** and **2_Fc** particles. UV-vis spectra of a dispersion of **1_Fc** in water clearly show two bands at around 300 and 450 nm against the background scattering, which are not visible in the case of **1_OH_g** (Figure 6B).

In addition, X-ray photoelectron spectroscopy (XPS) was used to confirm the presence of ferrocene on the SiO_2 particles. The high-resolution Fe 2p scan showed the presence of two

peaks at around 710 and 723 eV, which correspond to the $Fe2p_{1/2}$ and Fe $2p_{3/2}$ peaks (Figure 6C), which further demonstrates the success of the functionalization.[25]

Finally, electrochemical studies further confirmed the presence of Fc moieties on the particles. Cyclic voltammograms of dispersions of **1_Fc** in 0.1 M of $LiClO_4$ showed a typical reversible redox process with oxidation and reduction peaks that can be attributed to ferrocene (Figure 6D).[25]

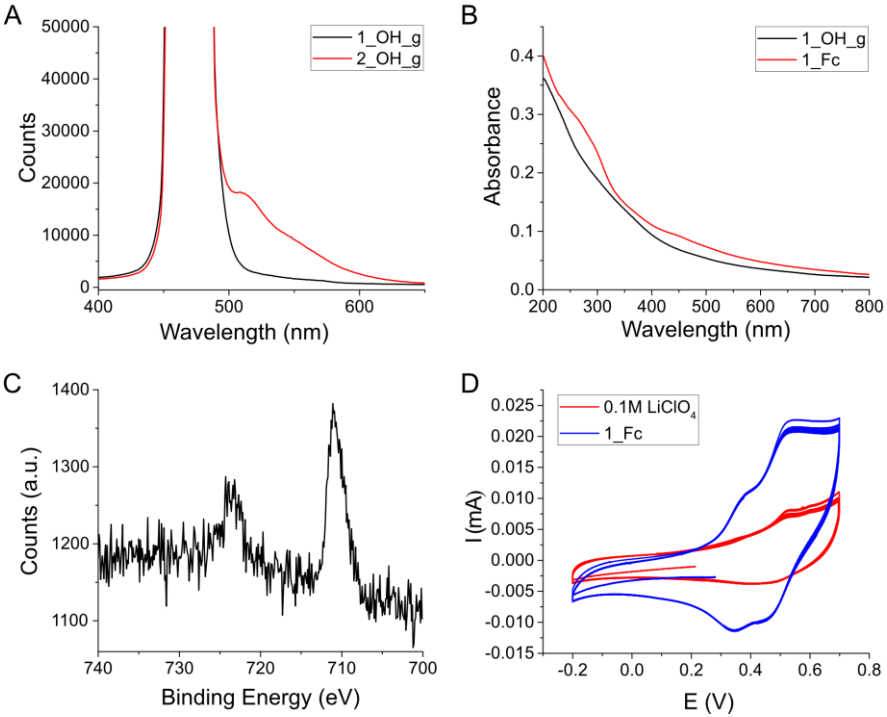

Figure 6. (A) Fluorescence spectra of ethanol dispersions of non-fluorescent **1_OH_g** and fluorescent **2_OH_g** silica particles. The large peak at 470 nm is from the excitation LED light; (B) UV-Vis spectra of 0.66 mg/mL water dispersions of **1_OH_g** and **1_Fc** SiO_2 particles. (C) High resolution XPS Fe 2p spectra of **1_Fc**; (D) Cyclic voltammogram of **1_Fc** in 0.1 M $LiClO_4$ (vs Ag/AgCl) at 0.1 V/s, compared to the voltammogram of a 0.1 M $LiClO_4$ water solution.

ζ-potential experiments were conducted to study the colloidal stability of the particles prepared at different stages of the functionalization. ζ-potential measurements provide information on the surface charges of the particles and thus can give further indication of the successful functionalization. We found values of ζ-potential of - 31.5 ± 0.6 mV for the bare SiO_2 particles, -19.9± 0.6 mV for azide-functionalized particles and -3.1 ± 0.3 mV for Fc-functionalized particles,

indicating a progressive decrease of the surface charge upon functionalization. This also correlates well with the colloidal stability visually observed for the measured solutions, with sedimentation occurring faster and more completely with the Fc-functionalized particles (Figure 7).

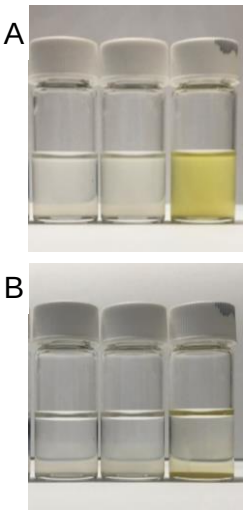

Figure 7. Colloidal stability of ethanol dispersions 0.67 mg/mL of (from left to right) bare, azide-functionalized, and Fc-functionalized particles: (A) as soon as dispersed; (B) after 24h.

5.3. REDOX STUDIES

Preliminary redox studies were performed using only ferrocene solutions, in order to find out the most suitable oxidant and reductant systems and to determine the number of equivalents required to achieve fast and reversible redox switching, as well as studying the redox kinetics. We performed these studies in a water/acetonitrile (8:2) solvent mixture which was a good compromise to dissolve both the ferrocene, sparingly soluble in pure water, and the β-CD-dimer, which is insoluble in organic solvents. However, we point out that this solubility issue does not affect the studies with Fc-functionalized particles since the Fc groups are carried on the surface of the colloid dispersed in aqueous solutions.

5.3.1. Oxidation studies

Ferrocene (Fc) oxidation was first studied by UV-Vis spectroscopy. The UV-Vis spectrum of ferrocene (reduced form) shows two characteristic bands at 326 and 440 nm (see Appendix 4). Upon oxidation of ferrocene to the ferrocenium ion (Fc^+), a new band appears at 618 nm in the visible spectrum, which corresponds to a color change of the Fc solution from the characteristic yellow to pale blue.

In previously reported studies, ferrocene and its derivatives have been oxidized using a variety of oxidants, including hydrogen peroxide, iron (III) chloride, potassium permanganate, silver nitrate, sodium hypochlorite and iodine, among others.[15] Therefore we chose to carry out a comparative study selecting some of these oxidants at different conditions, namely: H_2O_2 (in both neutral and acidic medium), $FeCl_3$ and commercial bleach (containing 2.5-5% NaClO). In a typical experiment, the oxidant was added to a 250 μM solution of Fc and the oxidation was followed by UV-Vis for approximately two days (in unstirred solutions).

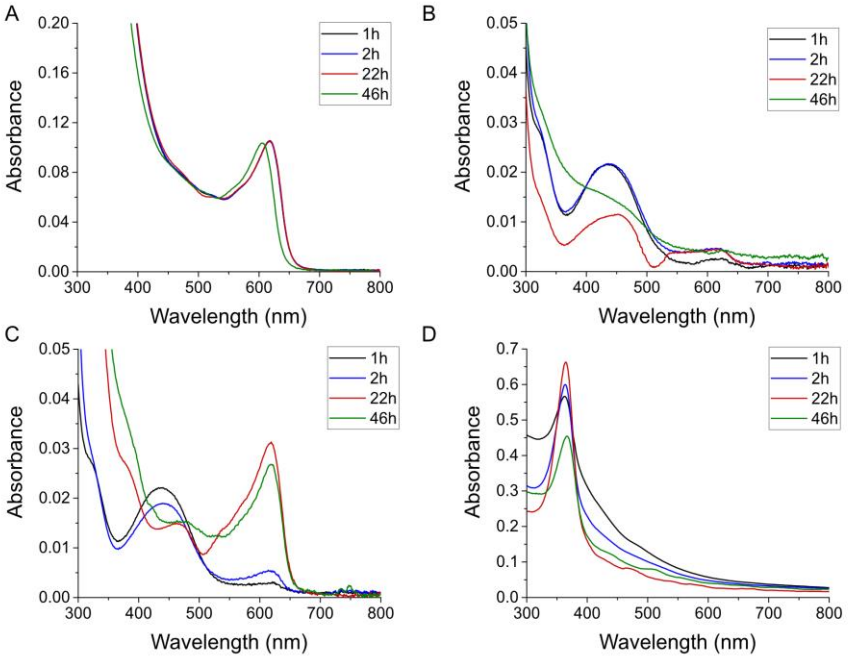

Figure 8. UV-Vis spectra of Fc oxidation with (A) 2 eq. of $FeCl_3$; (B) 10 eq. of H_2O_2; (C) 10 eq. of H_2O_2 in the presence of 1 eq. of CH_3COOH; (D) 2 eq. of commercial bleach. Note that in the case of $FeCl_3$ and bleach, the strong absorption below 450 nm due to the oxidant masks the Fc bands.

The different oxidants showed remarkably different behavior as observable in Figure 8. While the addition of 2 eq. of $FeCl_3$ was found to oxidize the Fc instantly, as shown by the sudden appearance of the band at 618 nm (Figure 8A), the full oxidation with H_2O_2 took place at a much slower rate over the course of two days. However, we found that the oxidation rate with H_2O_2 is strongly dependent on the pH of the solution, occurring much faster under acidic conditions, e.g. in the presence of 1 eq. of acetic acid (compare Figure 8B and C). This is interesting because it offers the possibility for further control and optimization of the oxidation kinetic, which is crucial in view of studying redox-controlled dissipative self-assembly. Finally, no oxidation peak was observed when using commercial bleach (Figure 8D), which was thus discarded as a potential oxidant for our system.

Following these initial results, we performed a kinetic study on the Fc oxidation process with H_2O_2 under acidic conditions (Figure 9A). This time, we also increased the number of equivalents of H_2O_2 from 10 to 65. In fact, we realized that in most redox-switchable supramolecular systems based on the Fc-β-CD host-guest interaction, when H_2O_2 is used as oxidant, a large excess of the peroxide with respect to Fc is always employed (up to 1500 equivalents or higher).[12]

Under these conditions the oxidation of Fc followed a sigmoidal behavior in which, after a short lag period, the oxidation rate (speed of Fc^+ formation) initially increases, reaches a maximum and then decreases until the concentration of Fc^+ reaches a plateau at around 15 hours (Figure 9B).

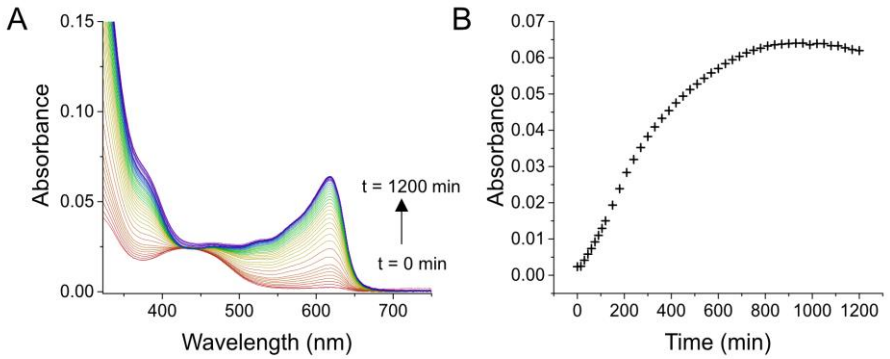

Figure 9. Kinetic study of Fc oxidation with 65 eq. of H_2O_2 in the presence of 1 eq. of CH_3COOH (A) Time-course measurement of the UV-Vis spectrum showing the appearance of the Fc^+ band; (B) absorbance of the ferrocenium peak at 618 nm over time.

5.3.2. Reduction studies

Like for the oxidation process, initial UV-Vis studies were performed to identify the best reductants to reduce the oxidized ferrocenium system. Two reductants were chosen for the study: glutathione (GSH) and ascorbic acid, since they have previously been reported as suitable reducing agents for the Fc/Fc^+ system.[15] To this aim, a 250 μM solution of ferrocene in water/acetonitrile (8:2) was first oxidized with $FeCl_3$ (2 eq.), followed by the addition of 5 equivalents of each reductant. The reaction was followed by UV-Vis for 30 mins (Figure 10). We observed that glutathione induced only a slight reduction of the Fc^+ absorption band over this time period (Figure 10A), whilst ascorbic acid reduced the oxidized Fc instantly (Figure 10B). For this reason, ascorbic acid, or sodium ascorbate (see below), were chosen as reductants for the system.

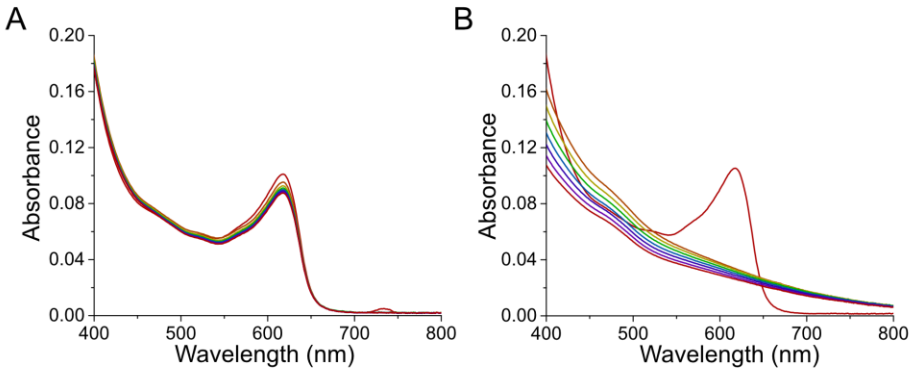

Figure 10. UV-Vis kinetics study of Fc reduction with (a) 5 eq. of GSH and (b) with 5 eq. of ascorbic acid.

5.3.3. Redox cycles

Once suitable oxidants and reductants had been identified, we then moved to study the possibility of performing multiple oxidation-reduction cycles through optimization of the reaction conditions.

Since the oxidation and reduction of the Fc/Fc^+ system by H_2O_2 and ascorbate respectively are strongly pH-dependent, and promote themselves a pH change along the course of the

reaction, we decided to follow the redox cycles by monitoring simultaneously the pH of the solution and the solution color. The latter changes from yellow to blue upon oxidation of Fc to Fc^+, as mentioned earlier. To this purpose we used a pH data logger and a color camera.

To a 250 µM solution of Fc (with 2 eq. of CH_3COOH) contained in a water/acetonitrile (8:2) mixture in a stirred vial, 65 eq. of H_2O_2 were added, which induced oxidation of Fc in about 3 hours. This corresponded to a gradual yellow to blue color change and to an increase of pH up to 4.72 (A to B in Figure 11). Afterwards, 2 equivalents of sodium ascorbate were added as a reductant, leading to a sharp increase of pH (mostly due to the basicity of the ascorbate) and instantaneous reduction of Fc^+, evidenced by an instantaneous change in color to yellow (B to C in Figure 11). Remarkably, after 80 min, the pH had returned to around the same value as before the reduction and the solution became blue again, indicating re-formation of Fc^+, despite no further addition of the oxidant (C to D in Figure 11). The redox cycle upon addition of the reductant could be repeated a further two times without needing to add additional oxidant. Afterwards, a large decrease of pH was observed, together with a loss of color and increase of turbidity of the solution (H in Figure 11), that can be ascribed to Fc degradation. Therefore, we demonstrated that, in the presence of an excess of H_2O_2 as oxidant, the system can be pushed transiently in its reduced state by batch addition of the reductant. This makes H_2O_2 and ascorbate suitable candidates to be used as chemical fuels to build redox-controlled DSA systems.

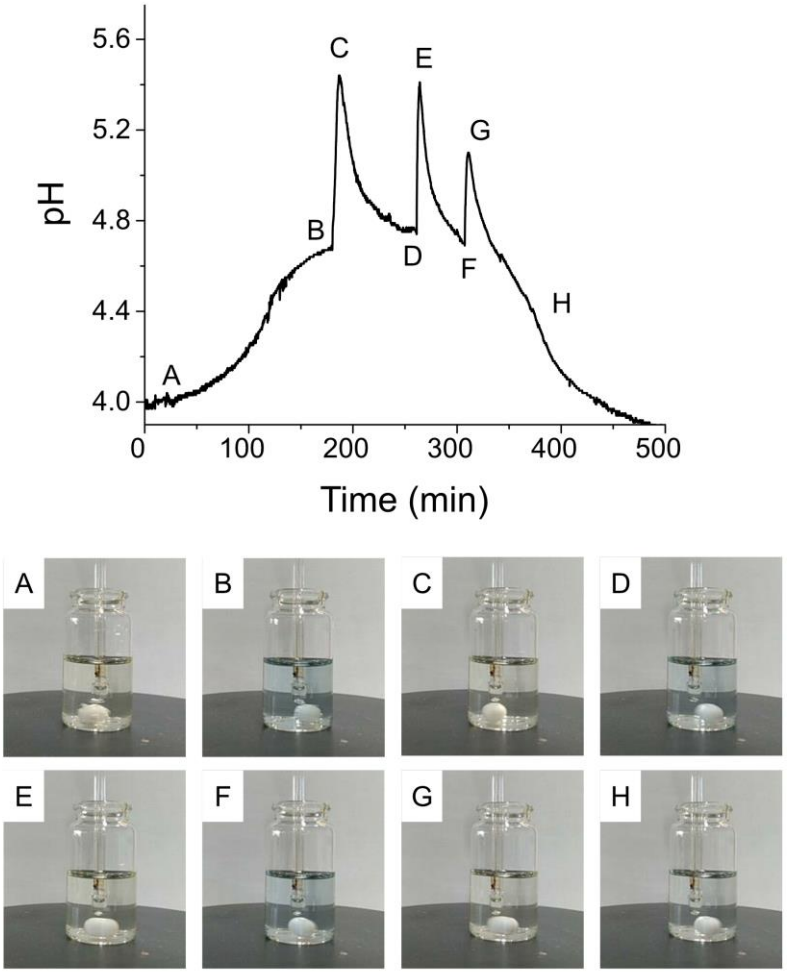

Figure 11. pH and color variation over time during redox cycles induced by batch additions of sodium ascorbate to a 250 µM solution of Fc (with 2 eq. of CH_3COOH) contained in a water/acetonitrile (8:2) in the presence of excess H_2O_2. (65 eq.)

5.4. SELF-ASSEMBLY STUDIES

Preliminary self-assembly studies were conducted with fluorescent Fc-functionalized SiO_2 particle solutions (**2_Fc**) by means of bright field and fluorescence microscopy. The particles were previously dispersed by sonication and vortexing in water and then placed into glass capillaries for imaging.

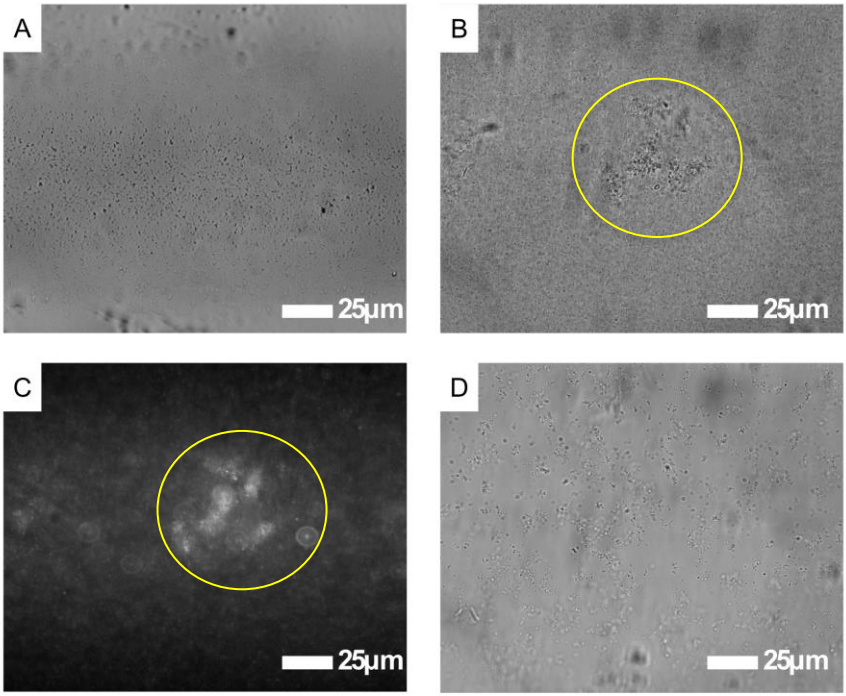

Figure 12. Bright field microscopy images of: (A) **2_Fc** SiO_2 particles; (B) **2_Fc** SiO_2 in the presence of β-CD-dimer; (D) solution as in B after $FeCl_3$ addition. (C) Fluorescence microscopy image corresponding to B.

Microscopy images show that Fc-functionalized particles remain well dispersed and isolated in solution in the absence of β-CD-dimer (Figure 12A) even after 24 hours, still showing significant Brownian motion. However, in the presence of an excess of the β-CD-dimer we observed the formation of several aggregates of colloidal particles, with diminished motion, accompanied by far fewer individual particles in solution (Figure 12B and Appendix 5). In addition, fluorescence imaging confirmed that the aggregates were in fact formed from the fluorescent particles (Figure 12C). Thus, the usage of fluorescent particles was key for the recognition of agglomerated matter.

Following the formation of these agglomerated structures, $FeCl_3$ was injected to promote disassembly. It was observed that the assembled structures were destroyed into oligomeric structures (Figure 12D). Further studies are currently being carried out to determine if the observed assembly and disassembly of the colloidal particles can indeed be ascribed to the complexation of the Fc-functionalized particles with the β-CD-dimer and to the Fc oxidation and subsequent disassociation, respectively. In fact, we cannot discard that the added species modify the stability of the colloidal system changing the particle surface energy by other mechanisms.

6. EXPERIMENTAL SECTION

6.1. MATERIALS AND METHODS

Tetraethyl orthosilicate, 3-aminopropyltriethoxysilane, fluorescein-isothiocyanate, ammonium hydroxide, absolute ethanol, 96% ethanol, dry toluene, sodium ascorbate, copper sulfate pentahydrate, isopropanol, ethylenediaminetetraacetic acid, ethynylferrocene, acetonitrile, commercial bleach, hydrogen peroxide, acetic acid, iron (III) chloride, ascorbic acid, sodium ascorbate and L-glutathione were obtained from commercial sources. Deionized or MilliQ water was used in experiments as indicated. 3-azidopropyltriethoxysilane and β-cyclodextrin-dimer were previously synthesized by other group members.

UV-Vis studies were performed using a Cary 60 Spectrometer. SEM images were obtained on a JEDL J-7100 Field Emission Scanning Electron Microscope. DLS measurements were made using a Cordouan VASCO KIN Particle Size Analyzer. The sparse Bayesian learning (SBL) algorithm was used for the Laplace transform inversion. Bright field and fluorescence microscopy images were obtained using a Nikon Eclipse Ti microscope using 40x and 60x objectives. FT-IR spectra were recorded on a Nicolet 6700 equipped with an ATR (Attenuated Total Reflectance) accessory. ζ-potential measurements were performed on a Malvern Zetasizer. Cyclic voltammetry was performed with a Biologic VSP-300 potentiostat. XPS experiments were performed in a PHI

5500 Multitechnique System (from Physical Electronics) with a monochromatic X-ray source (Aluminium Kalfa line of 1486.6 eV energy and 350 W).

6.2. PREPARATION OF FERROCENE-FUNCTIONALIZED SILICA PARTICLES

6.2.1. Synthesis of silica seeds

Fluorescent and non-fluorescent silica seeds were synthesized by following adapted literature procedures.[21]

Non-fluorescent silica seeds: 3-aminopropyltriethoxysilane (APTES) (100 µL, 0.43 mmol) was added to ethanol (5 mL), and the resulting solution sonicated for 5 minutes. To a 50 mL round bottom flask, 0.1 mL of this APTES solution and 0.878 mL of ammonia (28% in water) were added to 10 mL of ethanol. Under stirring, tetraethyl orthosilicate (TEOS) (0.4 mL, 1.76 mmol) was added under the meniscus to prevent secondary nucleation.[21] The reaction was then stirred at 300 rpm at room temperature for 17 h. The particles were washed with pure ethanol, sonicated, centrifuged at 3000 rcf for 30 min and the supernatant decanted. The washing protocol was repeated 3 times yielding a white powder that was dried at 70 ºC for 1h (180 mg).

Fluorescent silica seeds: A solution of dye-functionalized APTES was first prepared in a small vial by dissolving fluorescein isothiocyanate isomer I (10.5 mg, 0.03 mmol) in ethanol (0.5 mL). APTES (10 µl, 0.04 mmol) was then added to the solution. The mixture was stirred at 200 rpm at room temperature for 6 hours under Ar atmosphere, in the absence of light. To a 50 mL round bottom flask, the dye-functionalized APTES solution (0.1 mL) and 1.6 mL of ammonium hydroxide (28% in water) were added to 10 mL of ethanol, resulting in an ammonium hydroxide concentration of 1.96 M. TEOS (0.4 mL, 1.76 mmol) was then added under the meniscus of the stirred solution to prevent secondary nucleation. The reaction was stirred at 200 rpm at room temperature for 21 h. The particles were washed with pure ethanol, sonicated, centrifuged at 3000 rcf for 15 min and the supernatant decanted. This washing procedure was repeated 3 times with 15 mL ethanol each time, yielding a yellowish powder that was dried at 70 ºC for 1h.

6.2.2. Synthesis of core-shell silica particles

Core-shell silica particles were synthesized by following adapted literature procedures.[21]

Non-fluorescent and fluorescent silica particles: 3.1 mL of seed solution (6.55 mg/mL) were added to a solution of absolute ethanol (19 mL), dH_2O (6.34 mL) and ammonium hydroxide (28% in water) (1.27 mL) in a 250 mL round-bottom flask, which was then sealed and equipped with a continuous N_2 flow. Two 5 mL syringes were filled with: (1) a mixture of TEOS (1.87 mL) and ethanol (3.73 mL); (2) a mixture of 0.5 mL ammonium hydroxide (28% in water), 1.27 mL of dH_2O and 3.83 mL of ethanol. The syringes were connected to the flask with microfluidic Teflon tubing, and mounted on syringe pumps to control the addition of reactants. The flow rate was set at 1.2 mL/h, and the two solutions were infused over 3 h 30 min into the reaction flask. After complete addition, the reaction mixture was kept stirring at 200 rpm at room temperature overnight. The particles were washed with pure ethanol, sonicated, centrifuged at 3000 rcf for 15 min and the supernatant decanted. This washing procedure was repeated 3 times with 15 mL ethanol each time, and the particles were obtained as a white or yellowish powder that was dried at 70 ºC for 1h.

6.2.3. Functionalization of silica particles

Azide-functionalized and Fc-functionalized particles were derivatized following adapted literature procedures. The same protocol was used for non-fluorescent and fluorescent particles.

Azide-functionalized SiO_2 particles in ethanol (protocol 1a).[22] 3-azidopropyltriethoxysilane (10 µL, 0.04 mmol) was added to ethanol (990 µL) in an Eppendorf tube and sonicated for 1h. This solution was then added to a 10 mL round-bottom flask containing a suspension of non-fluorescent SiO_2 particles (13.6 mg/mL, 2 mL), under Ar atmosphere. The mixture was stirred at 300 rpm at room temperature for 22 h. The particles were separated by centrifugation, then washed with absolute ethanol, sonicated, centrifuged at 3000 rcf for 15 min and the supernatant decanted. This washing procedure was repeated 3 times with 15 mL ethanol each time.

Azide-functionalized SiO_2 particles in toluene (protocol 1b).[23] To a 10 mL round-bottom flask, non-fluorescent SiO_2 particles (54.4 mg) were added to dry toluene (4 mL) and 3-azidopropyltriethoxysilane (20 µL, 0.08 mmol) under Ar atmosphere. The reaction mixture was stirred at 300 rpm under reflux at 110 ºC for 20 h. After the mixture had cooled to ambient temperature, the particles were separated by centrifugation and the supernatant decanted. The particles were washed with acetone, sonicated, centrifuged at 3000 rcf for 15 min and the

supernatant decanted. This washing protocol was repeated 3 times with 15 mL acetone each time.

Fc-functionalized SiO_2 particles.[24] A solution of copper sulfate pentahydrate (4.6 mg, 0.018 mmol) in water (1 mL) was sonicated for 1h. A solution of non-fluorescent N_3-functionalized SiO_2 particles (23.3 mg) and isopropanol (3 mL) was added to a 10 mL round-bottom flask under Ar atmosphere. Ethynylferrocene (7.8 mg, 0.037 mmol), and the $CuSO_4$ solution previously prepared were added to the flask. Then, sodium ascorbate (7.2 mg, 0.036 mmol) was added to the solution. The mixture was stirred at 400 rpm at room temperature for 22 h. The particles were separated by centrifugation and the supernatant decanted. The particles were washed with a solution of EDTA (0.1M,15 mL), sonicated, centrifuged at 3000 rcf for 15 min and the solvent was decanted. The particles were then washed with water (2 x 15 mL) and ethanol (2 x 15 mL) and dried at 70 ºC for 1h yielding an orange solid.

6.3. PARTICLE SIZE CHARACTERIZATION

Preparation of SEM samples: Samples of silica seeds and core-shell particles in ethanol were deposited on a glass substrate. The glass substrates were firstly sonicated with acetone (1 x 15 min) and isopropanol (1 x 15 min). The substrates were then dried with N_2 gas. Samples of 6.55 mg/mL of the particles in ethanol were sonicated and dilutions of 1/10 and 1/100 were subsequently prepared in different vials. The drop casting was performed with 20 µL of the concentrated and diluted samples for 20 seconds. After that, N_2 gas was applied to completely dry the sample.

6.4. REDOX STUDIES

6.4.1. Oxidation studies

Stock solutions: A 100 mM Fc solution was prepared in acetonitrile and filtered to remove any particulate impurities. 100 mM oxidant solutions of H_2O_2, $FeCl_3$ and commercial bleach (2.5-5% NaClO), as well as a 100 mM acetic acid solution, were prepared in water.

Sample preparation: 7.5 µL of 100 mM Fc stock solution was added to 3 mL 8:2 dH_2O/CH_3CN solvent mixture to yield a solution with Fc concentration 250 µM. To these sample

solutions, the oxidant stock solutions were added in the following amounts: NaClO (2 eq.), $FeCl_3$ (2 eq.), H_2O_2 (10 eq.) and H_2O_2 (10 eq.) + CH_3COOH (1 eq.). The samples were kept at 25 ºC between measurements.

For the kinetic study, 7.5 µL of 100 mM Fc stock solution was added to acetonitrile (0.6 mL) in a quartz cuvette. Deionized water (2.4 mL) was then added to obtain an 8:2 dH_2O/CH_3CN solvent mixture. It was important to add Fc to CH_3CN first, followed by the addition of water to prevent Fc precipitation. 7.5 µL of 100 mM CH_3COOH stock solution (1 eq.) and 5 µL of a concentrated 9.8 M H_2O_2 solution (65 eq.) were added to the quartz cuvette.

6.4.2. Reduction studies

Stock solutions: A 100 mM Fc solution was prepared in acetonitrile and filtered to remove any particulate impurities. 100 mM reductant solutions of GSH, ascorbic acid, and sodium ascorbate as well as a 100 mM acetic acid solution, were prepared in water.

Sample preparations: 7.5 µL of 100 mM Fc stock solution was added to 3 mL 8:2 dH_2O/CH_3CN solvent mixture to yield a solution with Fc concentration 250 µM. The corresponding reductants: GSH (5 eq.) or ascorbic acid (5 eq.) were then added to the Fc solution for UV-Vis studies.

For the redox cycling experiment monitored by pH, 22.5 µL of 100 mM Fc stock solution was added to CH_3CN (1.8 mL) and dH_2O (7.2 mL) to yield a solution with Fc concentration 250 µM. Acetic acid (2 eq.) and H_2O_2 (65 eq.) were added to the solution to oxidize the ferrocene and the solution was stirred at 185 rpm. Batches of sodium ascorbate (2 eq.) were subsequently added, and the initial reduction followed by slow oxidation were followed by monitoring the pH and color change of the solution.

6.5. SELF-ASSEMBLY STUDIES

Stock solutions: 1 mM β-CD-dimer and 100 mM $FeCl_3$ solutions were prepared in water.

Sample preparations: Fluorescent Fc functionalized particles (**2_Fc**) were used for self-assembly studies. A dispersion of **2_Fc** in Milli-Q water (250 µg/mL) was sonicated for 1 h and transferred to a clean glass capillary.

To 20 µL dispersion of **2_Fc** in Milli-Q water (250 µg/mL), 5 µL of a β-CD-dimer solution (1 mM) in water was added in an Eppendorf. The sample was sonicated for 30 min and transferred to a clean glass capillary.

7. CONCLUSIONS

In conclusion, in the current TFG project we have:

- Successfully synthesized non-fluorescent and core-shell fluorescent SiO_2 particles through the Stöber method;
- Obtained control over SiO_2 particle size by using a two-step synthetic protocol. Size and morphology characterization by DLS and SEM, revealed the formation of monodisperse spherical particles of around 500 nm diameter;
- Successfully functionalized the SiO_2 particles with Fc via a two-step procedure using 'click' chemistry. UV-Vis, XPS and CV demonstrated the presence of Fc at the particle surface.
- Demonstrated the fluorescence of the obtained SiO_2 particles, by using fluorescence spectroscopy and microscopy;
- Identified the best oxidant and reductant systems for Fc/Fc^+ and optimized the experimental conditions for controlling the redox kinetics (studied by UV-Vis and changes in pH). We found that $FeCl_3$ and ascorbic acid (or sodium ascorbate) are the most suitable redox agents for fast redox switching of Fc/Fc^+, whilst H_2O_2 enables the control of the redox kinetics depending on the pH (with faster oxidation observed under acidic conditions);
- Demonstrated that, in the presence of an excess of H_2O_2 as oxidant, batch additions of ascorbate can push the Fc/Fc^+ system transiently to its reduced state, which is a very important result in view of building redox-controlled colloidal DSA systems;
- Obtained preliminary results showing the colloidal assembly of the Fc-functionalized SiO_2 in the presence of the β-CD dimer, and its disassembly upon addition of $FeCl_3$. Further studies have to be carried out to investigate the system in more depth.

8. REFERENCES AND NOTES

1. De, S. & Klajn, R. Dissipative Self-Assembly Driven by the Consumption of Chemical Fuels. *Adv. Mater.* **30**, 1706750 (2018).
2. van Ravensteijn, B. G. P., Voets, I. K., Kegel, W. K. & Eelkema, R. Out-of-Equilibrium Colloidal Assembly Driven by Chemical Reaction Networks. *Langmuir* **36**, 10639–10656 (2020).
3. Rossum, S. A. P. van, Tena-Solsona, M., Esch, J. H. van, Eelkema, R. & Boekhoven, J. Dissipative out-of-equilibrium assembly of man-made supramolecular materials. *Chem. Soc. Rev.* **46**, 5519–5535 (2017).
4. Grzelczak, M., M. Liz-Marzán, L. & Klajn, R. Stimuli-responsive self-assembly of nanoparticles. *Chem. Soc. Rev.* **48**, 1342–1361 (2019).
5. Vilanova, N., Feijter, I. de, Teunissen, A. J. P. & Voets, I. K. Light induced assembly and self-sorting of silica microparticles. *Sci. Rep.* **8**, 1271 (2018).
6. Klajn, R., Wesson, P. J., Bishop, K. J. & Grzybowski, B. A. Writing self-erasing images using metastable nanoparticle "inks". *Angew. Chem. Int. Ed.* **48**, 7035–7039 (2009).
7. van Ravensteijn, B. G. P., Hendriksen, W. E., Eelkema, R., van Esch, J. H. & Kegel, W. K. Fuel-Mediated Transient Clustering of Colloidal Building Blocks. *J. Am. Chem. Soc.* **139**, 9763–9766 (2017).
8. Ma, X. & Zhao, Y. Biomedical Applications of Supramolecular Systems Based on Host–Guest Interactions. *Chem. Rev.* **115**, 7794–7839 (2015).
9. Komiyama, M. & Bender, M. L. Chapter 14 Cyclodextrins as enzyme models. in *New Comprehensive Biochemistry* vol. 6 505–527 (Elsevier, 1984).
10. Harada, A., Takashima, Y. & Nakahata, M. Supramolecular Polymeric Materials via Cyclodextrin–Guest Interactions. *Acc. Chem. Res.* **47**, 2128–2140 (2014).
11. Shi, W. *et al.* Redox-responsive polymeric membranes via supermolecular host–guest interactions. *J. Membr. Sci.* **480**, 139–152 (2015).
12. Facciotti, C. *et al.* Oxidant-responsive ferrocene-based cyclodextrin complex coacervate core micelles. *Supramol. Chem.* **32**, 30–38 (2020).
13. Peng, L., Feng, A., Huo, M. & Yuan, J. Ferrocene-based supramolecular structures and their applications in electrochemical responsive systems. *Chem Commun* **50**, 13005–13014 (2014).
14. Yan, Q., Feng, A., Zhang, H., Yin, Y. & Yuan, J. Redox-switchable supramolecular polymers for responsive self-healing nanofibers in water. *Polym. Chem.* **4**, 1216–1220 (2013).
15. Gu, H. *et al.* Redox-stimuli-responsive drug delivery systems with supramolecular ferrocenyl-containing polymers for controlled release. *Coord. Chem. Rev.* **364**, 51–85 (2018).
16. Liu, X., Zhao, L., Liu, F., Astruc, D. & Gu, H. Supramolecular redox-responsive ferrocene hydrogels and microgels. *Coord. Chem. Rev.* **419**, 213406 (2020).
17. Nakahata, M., Takashima, Y., Yamaguchi, H. & Harada, A. Redox-responsive self-healing materials formed from host–guest polymers. *Nat. Commun.* **2**, 511 (2011).

18. Stöber, W., Fink, A. & Bohn, E. Controlled growth of monodisperse silica spheres in the micron size range. *J. Colloid Interface Sci.* **26**, 62–69 (1968).
19. Greasley, S. L. *et al.* Controlling particle size in the Stöber process and incorporation of calcium. *J. Colloid Interface Sci.* **469**, 213–223 (2016).
20. Plumeré, N., Ruff, A., Speiser, B., Feldmann, V. & Mayer, H. A. Stöber silica particles as basis for redox modifications: Particle shape, size, polydispersity, and porosity. *J. Colloid Interface Sci.* **368**, 208–219 (2012).
21. Vilanova, N., De Feijter, I. & Voets, I. K. Synthesis and Characterization of Supramolecular Colloids. *J. Vis. Exp.* 53934 (2016) doi:10.3791/53934.
22. Graf, C. *et al.* Surface Functionalization of Silica Nanoparticles Supports Colloidal Stability in Physiological Media and Facilitates Internalization in Cells. *Langmuir* **28**, 7598–7613 (2012).
23. Zhang, G., Wang, Y., Wen, X., Ding, C. & Li, Y. Dual-functional click-triazole: a metal chelator and immobilization linker for the construction of a heterogeneous palladium catalyst and its application for the aerobic oxidation of alcohols. *Chem. Commun.* **48**, 2979 (2012).
24. Ciampi, S., Le Saux, G., Harper, J. B. & Gooding, J. J. Optimization of Click Chemistry of Ferrocene Derivatives on Acetylene-Functionalized Silicon(100) Surfaces. *Electroanalysis* **20**, 1513–1519 (2008).
25. Ling, X. Y., Reinhoudt, D. N. & Huskens, J. Ferrocenyl-Functionalized Silica Nanoparticles: Preparation, Characterization, and Molecular Recognition at Interfaces. *Langmuir* **22**, 8777–8783 (2006).

9. ACRONYMS

APTES	3-aminopropyltriethoxysilane
ATP	adenine triphosphate
ATR	Attenuated Total Reflectance
BTA	benzene-1,3,5-tricarboxamide
CD(s)	cyclodextrin(s)
CuAAC	copper catalyzed azide-alkyne cycloaddition
CV	Cyclic Voltammetry
d_H	hydrodynamic diameter
dH_2O	deionized water
DLS	Dynamic Light Scattering
DSA	Dissipative Self-Assembly
EDTA	ethylenediaminetetraacetic acid
Fc	ferrocene
GSH	glutathione
IR	Infra-Red
k_a	association constant
PDI	Polydispersity Index
rcf	relative centrifugal force
rpm	revolutions per minute
SBL	sparse Bayesian learning
SEM	Scanning Electron Microscopy
TEOS	tetraethyl orthosilicate
UV-Vis	Ultraviolet-Visible

XPS	X-ray Photoelectron Spectroscopy

APPENDICES

APPENDIX 1: SEM IMAGES

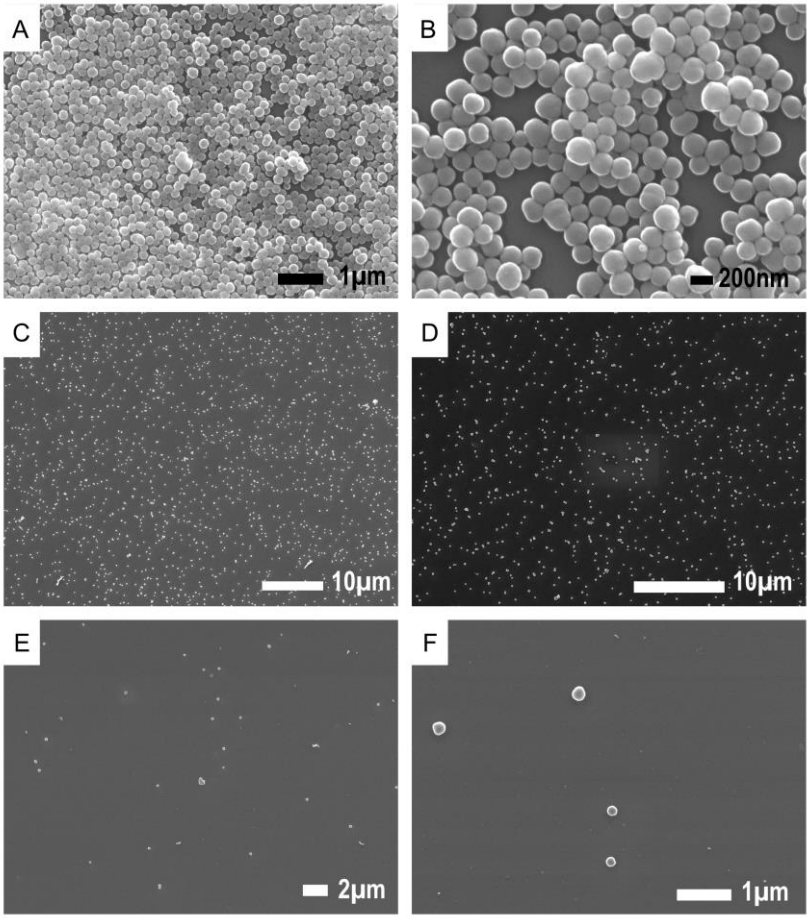

SEM images of seeds of the fluorescent SiO_2 particles (**2_OH_s**). Samples were drop cast on glass at different concentrations. (A,B) 6.55 mg/mL in ethanol; (C,D) 0.65 mg/mL in ethanol, (E,F) 0.065 mg/mL in ethanol.

APPENDIX 2: PARTICLE SIZE DISTRIBUTION

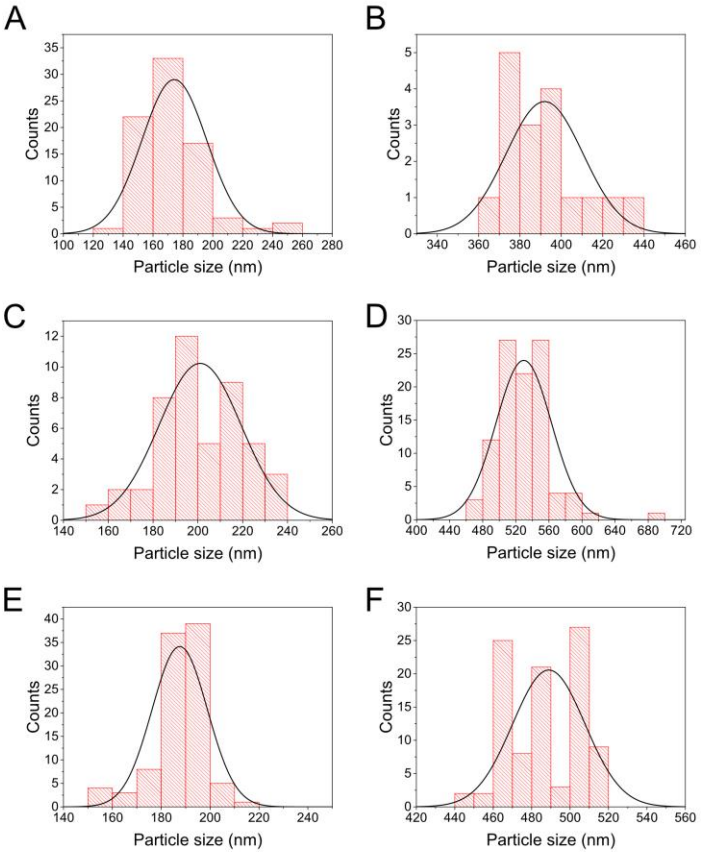

Particle size distribution histograms of (A) **1_OH_s**; (B) **1_OH_g**; (C) **fluo_OH_s**; (D) **fluo_OH_g**; (E) **2_OH_s**; (F) **2_OH_g**.

APPENDIX 3: IR SPECTRA

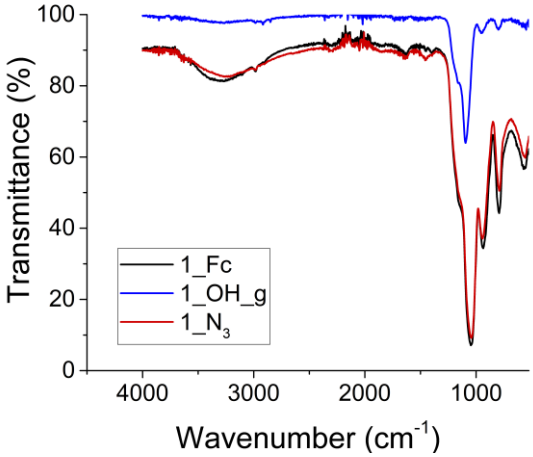

FT-IR spectra of grown SiO_2 particles (**1_OH_g**), azide-functionalized SiO_2 particles (**1_N_3**) and Fc-functionalized SiO_2 particles (**1_Fc**).

APPENDIX 4: UV-VIS SPECTRUM OF FC

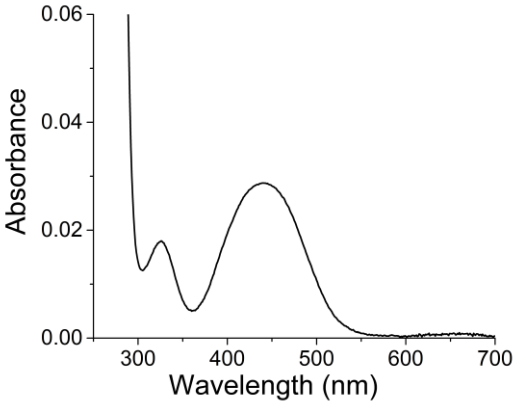

UV-Vis spectrum of Fc (250 μM) solution in H_2O/CH_3CN (8:2) mixture.

APPENDIX 5: BRIGHT FIELD MICROSCOPY IMAGES

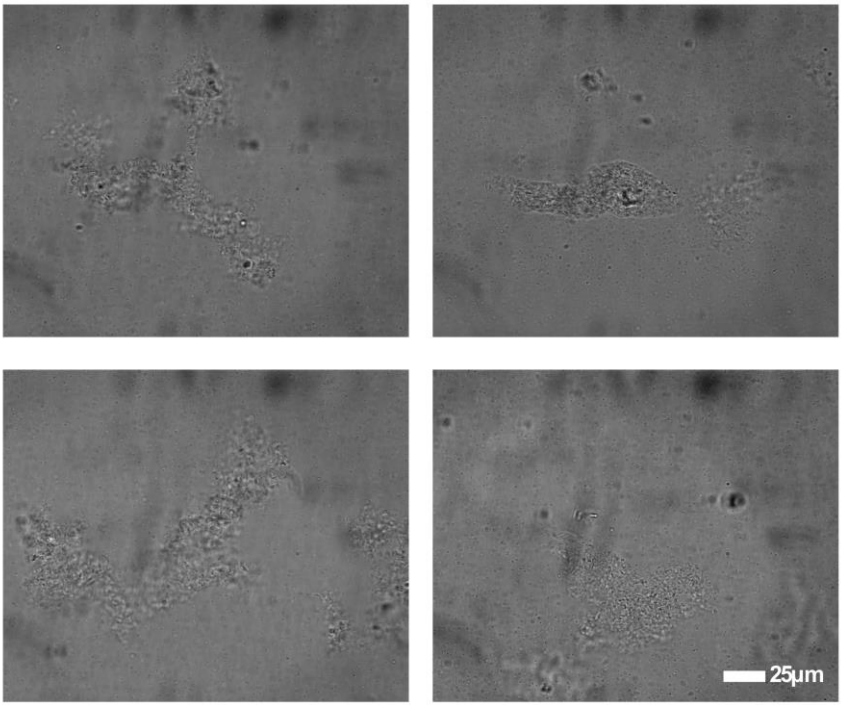

Bright field images of **2_Fc** SiO_2 particles in the presence of β-CD-dimer.